This article has been accepted for publication in a future issue of this journal, but has not been fully edited. Content may change prior to final publication. Citation information: DOI 10.1109/TNB.2019.2958891, IEEE Transactions on NanoBioscience

Development of Uric Acid Biosensor using Gold Nanoparticles and Graphene Oxide Functionalized Micro-Ball Fiber Sensor Probe

Santosh Kumar, *Senior Member*, *IEEE*, Ragini Singh, Guo Zhu, Qingshan Yang, Xia Zhang, Shuang Cheng, Bingyuan Zhang, Brajesh Kumar Kaushik, *Senior Member*, *IEEE*, Feng-Zhen Liu

***Abstract*— A highly sensitive and selective optical fiber-based enzymatic biosensor has been proposed in the present study for detection of uric acid (UA) in human serum. The working mechanism of sensor depends on surface plasma property and localized surface plasmon resonance technique. For this purpose, a micro-ball fiber sensor probe of 350 µm diameter was fabricated using advanced fusion-splicer and coated with gold nanoparticles (AuNPs) and graphene oxide (GO) in order to enhance its sensitivity. UV-Visible spectrophotometer and high-resolution transmission electron microscope (HR-TEM) were used to characterize the AuNPs solution and GO aqueous dispersion. The absorbance spectrum of AuNPs and GO are recorded at 519 nm and 230 nm, respectively. The coating of AuNPs and GO over fiber surface were verified by using a scanning electron microscope (SEM) and energy-dispersive X-ray spectroscopy (EDX). Thereafter, sensor probe was functionalized with the specific enzyme i.e. uricase for the UA detection. The linearity response of uricase/GO/AuNPs-coated micro-ball optical fiber sensor is reported in the range of 10 µM – 1 mM UA concentrations. The reflectance of sensor linearly decreases with the increasing UA concentrations. Sensitivity of the sensor is 2.1 %/mM with a good slope of linearity with detection limit of 65.60 µM. To test the accuracy of proposed sensor, UA concentration in serum samples have also tested by using proposed sensor and A5800 Automatic Biochemical Analyzer. The results of the developed sensor are consistent with the results of A5800 Automatic Biochemical Analyzer. Thus, proposed sensor can be successfully utilized for UA detection in human serum samples.**

***Index Terms*— Uric acid, serum, micro-ball fiber structure, gold nanoparticles, graphene oxide, uricase, localized surface plasmon resonance.**

I. Introduction

Uric acid (UA) is a vital product of purine metabolism and very important biomolecules found in human serum and urine [1]. A normal range of UA concentration in human serum (blood) has been reported in the range of 100 - 400 µM [2]. The dearth of exercise, deleterious diet, and fallacious drugs increases the UA concentration in blood. An excessive amount of UA in human body form solid-state urate and causes severe disease such as gout or kidney stones [3]. The elevated level of UA in human serum also causes many disorders such as renal failure, hyperuricemia, physiological disorder, stroke, high cholesterol, cardiovascular diseases, multiple sclerosis, and myocardial infarction [1-3]. Till now, there are several biosensors based on electrochemical [2, 4], colorimetric [5], fluorescence [3, 6, 7], and optical [8-10] techniques were developed for UA detection. Enzymatic based electrochemical sensors work on the principle of UA oxidation in the presence of uricase enzyme, which produces allantoin and hydrogen peroxide (H_2O_2) as byproducts [2, 4]. But, these sensors have based on the chemical oxidation process thus, suffers from some major drawbacks such as, require more time for detection and low sensitivity. Wang *et al.* [5] have developed a 3,3′,5,5′-tetramethylbenzidine (TMB)-based colorimetric probe for UA detection. This sensor is based on the redox reaction of TMB and $HAuCl_4$ with different concentrations of UA. But, linear response of the sensor lies in narrow range 0.001- 80.0 µM i.e., below than normal UA range in human beings. Xu *et al.* [3] developed an UA sensor using gold nanoclusters (AuNCs) that work on fluorescence technique for linear range of 0.7 - 80 µM and detection limit of 120 nM. Thereafter, Wang *et al.* [7] developed gold/silver nanoclusters (Au/AgNCs) based fluorescence sensor for UA detection in the range of 5 - 50 µM with detection limit of 5.1 µM. The detection range of these sensors are also low, therefore these sensors cannot be used directly for hyperuricemia patients. Wang *et al.* [6] developed gold nanoclusters (AuNCs) based fluorescence sensor for UA detection in the range of 10 - 800 µM with a detection limit of 6.6 µM. Rana *et al.* [11] developed the surface acoustic wave (SAW) technique based enzymatic sensor using zinc oxide

This work was supported by the National Key Research & Development program of China (2016YFB0402105), the Belt and Road Special Project approved by Shandong province for Introduction of Foreign Experts in 2018, and Liaocheng University, China (31805180301, 31805180326).

(Corresponding author: Santosh Kumar and Bingyuan Zhang)

S. Kumar, G. Zhu, Q.-S. Yang, X. Zhang, and B. Zhang are with the Shandong Key Laboratory of Optical Communication Science and Technology, School of Physics Science and Information Technology, Liaocheng University, Liaocheng-252059, Shandong, China. (email: santosh@lcu.edu.cn; 2902831435@qq.com; 834216805@qq.com; wenerzhang2002@163.com; zhangbingyuan@lcu.edu.cn)

R. Singh, and S. Cheng are with the School of Agriculture Science, Liaocheng University, Liaocheng-252059, Shandong, China. (e-mail: singh@lcu.edu.cn; chengshuang@lcu.edu.cn).

B. K. Kaushik is with the Department of Electronics and Communication Engineering, Indian Institute of Technology Roorkee, Roorkee-247667, Uttarakhand, India (e-mail: bkk23fec@iitr.ac.in).

F.-Z. Liu is with the Liaocheng People's Hospital, Medical College of Liaocheng University, Liaocheng, 252000, China (e-mail: ldcllfz@163.com).

(ZnO) thin film for UA detection. Misra *et al.* [8] also developed LSPR based optical probe for UA detection. They have detected the UA in bovine and human serum samples. In these works, reproducibility, reusability, and selectivity need to be discussed in detail for further improvement. Now a days, optical fiber-based sensors have proved to be more beneficial in terms of compactness, low cost, narrow resonance peaks with high sensitivity and stability, flexible design, miniaturized sensor, and capability of remote sensing [12]. These sensors are also immune to corrosion and electromagnetic interference (EMI) [9]. Lokman *et al.* [9] developed the optical fiber sensor (OFS) using ZnO nanowires coated - inline Mach-Zehnder interferometer (MZI) for UA detection. Moreover, Batumalay *et al.* [10] also developed ZnO nanostructures coated tapered plastic OFS for the detection of UA. Although, these sensors were works on the principle of surface plasmon resonance (SPR)/ localized surface plasmon resonance (LSPR). But there is a limited discussion about the sensitivity and usability of sensor probe for UA detection in human serum/urine. Considering these limitations, it is essential to develop a highly sensitive and selective biosensor for UA detection in human serum samples. SPR/LSPR based biosensors are quite simple, operate in real-time, highly sensitive, and measurement of sample can be done without prior treatment [8]. LSPR technique is highly sensitive to the biomolecules present around the nanoparticles (NPs) that plays an important role in the detection. Till now, several nanomaterials such as Fe_2O_3 NPs [2], quantum dots [3], graphene films [4], gold nanoclusters (AuNCs) [6], Zinc oxide (ZnO) nanowires [9], ZnO nanostructures [13], silver nanoparticles (AgNPs) [8], and Au nanoplates [14] have been effectively employed for the UA detection. Gold nanoparticles (AuNPs) [15] is the most sensitive nanoparticle among all because it exhibits the intrinsic biological peroxidase-like activity due to unique chemical, electronic and physical properties. These activities can be used in development of biosensors [16, 17]. However, biomolecules are poorly absorbed over AuNPs that limits its sensitivity. In order to improve the sensitivity of biosensors, a new sensing material graphene oxide (GO) is used that demonstrates unique optical property and ability to absorb the biomolecules [18]. GO is a nonmetal material and has special surface plasmon property. In OFSs, GO is coated over the surface of optical fiber to get an evanescent wave (EW) through GO [18]. Till now, MZI [9], and tapered fiber [13] structures were used to develop the optical fiber-based UA sensor. Here, fiber ball structure is used to develop the LSPR based OFSs. The fiber ball structure is miniature, stable, high sensitive OFS probe and its fabrication cost are also low [19-21]. Song et al. [21] reported a microsurgical sensor using fiber optic ball lens for the optical coherence tomography. Furthermore, Fuglerud et al. [22] reported the fiber ball sensor for monitoring the glucose level in diabetics.

In the present work, we demonstrate the two sensor probes, (i) uricase/AuNPs- coated, (ii) uricase/GO/AuNPs-coated micro-ball fiber sensor for UA detection in human serum samples. GO combined with the AuNPs is the uniqueness of this sensor probe. Thus, surface plasma property of GO and LSPR property of AuNPs in combination increases the sensitivity of sensor. Fiber micro-ball structure is a sensitive probe and able to detect even a single drop of solution due to its micro-size. Section II describes the materials and methods for the fabrication of sensor probe. Section III consists of the results, analysis and performance comparison of the sensor. Section IV concludes the work.

II. Materials and Methods

A. Materials

Graphite powder, sodium nitrate, sulphuric acid, potassium permanganate, hydrogen peroxide, and hydrochloric acid were used to synthesis of GO. Hydrogen tetrachloroaurate ($HAuCl_4$), trisodium citrate, hydrogen peroxide (H_2O_2), sulfuric acid, and (3-mercaptopropyl) trimethoxysilane (MPTMS) were used for AuNPs synthesis and coating process. Uricase (U0880, Sigma-Aldrich), phosphate-buffered saline (PBS), N-(3-Dimethylaminopropyl)-N′-ethylcarbodiimide hydrochloride (EDC), N-Hydroxysuccinimide (NHS), and 11-Mercaptoundecanoic acid (MUA) were used for enzyme functionalization. Uric acid (U2625, Sigma-Aldrich), D-glucose, glycine, L-alanine, L-proline, β-cyclodextrin, and L-glutathione were used for measurement and selectivity test of sensor probe. Most of the reagents were of analytical grade and were purchased from Sigma – Aldrich (Shanghai, China). These reagents were used in the experiment without any further purification. All aqueous solutions were prepared using deionized (DI) water of specific resistivity of 18 MΩcm.

B. Fabrication of micro-ball fiber structure

The standard single-mode fiber (SMF) was used to fabricate a micro-ball fiber structure because mode interfering noise is low in SMF [19-21]. The narrow core diameter (9 μm) and single-mode in SMF eliminate the distortion and attenuation that mainly occur due to multiple modes. The micro-ball fiber structure was fabricated using ball splicing mode of advanced fusion-splicer (FSM-100 P+ ARC Master, Fujikura, Japan) as per schematic shown in Fig. 1. For fabrication, coating of the fiber was removed using stripper and fiber clamp was used to hold the fiber on the V-groove. After placing the fiber, micro-ball structure was fabricated using arching process. We have used the optimized parameters such as adjustment of electrode 0 μm, pre-heat time 0 sec, cleaning arc time 150 ms, and electrode gap 2.2 mm in the fusion splicer. The tip of the fiber absorbed the arc discharging and heated. The melting part of the fiber turns into spherical shaped. To avoid the misalignment, the fiber was rotated during the tip solidification [20]. The proposed fiber sensor works on two-beam interference principle as shown in Fig. 1. The optical interference equation can be written as [20],

$$I = I_1 + I_2 + 2\sqrt{I_1 I_2}\cos(\Delta\emptyset) \quad (1)$$

where $\Delta\emptyset$ is the optical path length difference between beam I_1 and I_2.

$$\Delta\emptyset = \frac{4\pi}{\lambda} n_d d \quad (2)$$

where, n_d is the refractive index (RI) of UA solution and d is the distance between the fiber ball and surface of UA solution,

This article has been accepted for publication in a future issue of this journal, but has not been fully edited. Content may change prior to final publication. Citation information: DOI 10.1109/TNB.2019.2958891, IEEE Transactions on NanoBioscience

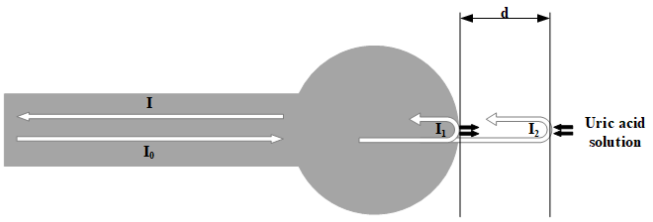

Fig. 1. Schematic of micro-ball fiber structure.

and λ is the wavelength of input optical signal. The EW inside fiber ball structure also plays an important role in the sensing of UA solutions. The EW exponentially decays as a function of radius of the fiber. The strength of the evanescent field depends on several factors like RI of core, RI of UA solution, core radius, and operating wavelength. The penetration depth is expressed as [23]

$$d_p = \frac{\lambda}{2\pi\sqrt{n_{cl}^2 \sin^2\theta - n_{ua}^2}} \quad (3)$$

where λ is the wavelength of a light source, θ is angle of incidence of the light at the cladding and UA solution interface, n_{cl} and n_{ua} are RIs of cladding and UA solution, respectively. Due to circular symmetry of SMF, two supermodes are excited in core by the fundamental mode [24]. These supermodes play an important role in sensing. Here, AuNPs are coated over the cladding surface of fiber ball structure. The intensity (I) on the AuNPs-coated cladding surface is given by [25]:

$$I = \frac{F_{ab} n_{eff} c}{\varepsilon_C \beta \alpha''} \quad (4)$$

where, F_{ab} is the absorption force on the AuNPs. n_{eff} is the effective index, β is the modal propagation constant. ε is the permittivity of the medium surrounding the AuNPs, α'' is the imaginary part of polarizability, c is the speed of light in vacuum. Sensitivity of detection 'S' can be analyzed as [25];

$$S = \varepsilon L \left(\eta + C\frac{dn}{dC}\right) \quad (5)$$

where dn/dC is the variation of RI of different UA concentration, ε is the molar absorptivity; C is the concentration of UA. L is the length of interaction and η is evanescent power factor. Here, η, F_{ab} is directly proportional to I. F_{ab} can be maximum for smaller size of AuNPs. As F_{ab} will be more, maximum evanescent field will come out from the cladding surface of fiber ball structure that increases the sensitivity of sensor.

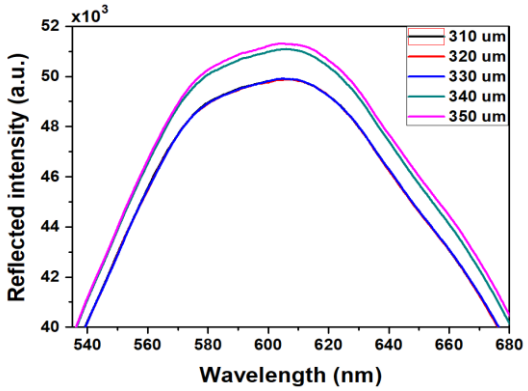

Fig. 2. Measurement of reflected intensities through different micro-ball fiber structure.

To realize the suitable micro-ball structure, five micro-ball of different diameters 310, 320, 330, 340, and 350 µm were fabricated. Then, reflected intensities were measured using different micro-ball structures. It can be observed from Fig. 2 that, reflection intensity is higher in the case of 350 µm diameter of fiber ball structure. So, in further study, fiber ball of 350 µm diameter was used for the development of UA sensor probe.

C. Synthesis of gold nanoparticles and graphene oxide

AuNPs were synthesized with the help of Turkevich method as discussed in [26]. For the AuNPs synthesis, chloroauric acid (150 µL, 100 mM) was added into 14.85 ml of DI water then solution was heated until boil. Thereafter, trisodium citrate (1.8 ml, 38 mM) was instantly added with vigorous stirring. The red color solution of AuNPs was obtained after 10 minutes. This solution was used in an experiment without further purification.

GO was synthesized using modified Hummer's method as discussed in [27, 28]. Firstly, 0.5×10^{-3} kg of graphite powder was mixed with 0.25×10^{-3} kg of sodium nitrate in 11.5 ml of sulphuric acid and stirred for 1 hr. Thereafter, 1.5×10^{-3} kg of potassium permanganate was slowly added in the solution by keeping the temperature of solution less than 20°C to avoid overheating and explosion. Then, mixture was stirred at 35°C for 2 hrs, and diluted with 250 ml of DI water and kept at 98°C for 15 minutes to obtain the brown color of solution. Thereafter, 2.5 ml of H_2O_2 was added to terminate the reaction. Further, solution was diluted with 250 ml of warm water to obtain the yellow color solution that confirms the formation of GO. Then, the solution was filtered by centrifugation through which particles settle at the bottom and remaining water was removed away. The resulting solution was washed twice with 5% hydrochloric acid (HCl) and then twice with DI water to obtain a gel solution. HCl helps to remove the sulfate ions and water removes the chloride ions from the GO solution [27]. It also helps to get the neutral pH of the solution. Gel-like substance was dried at 60°C for more than 6 hrs. Thereafter, GO powder was obtained by meshing the dried substance-using pestle mortar.

D. Characterization

Ultraviolet-visible (UV-Vis) spectrophotometer (HITACHI-U-3310) was used to measure the absorption spectrum of AuNPs and GO aqueous dispersion. GO powder was dispersed in de-ionized (DI) water by sonicating it for 20 min. The dispersed solution of GO was used to measure the absorbance spectrum taking water as a reference. UV-Vis spectrum confirmed that GO aqueous dispersion contained a large number of single-layered GO sheets [29, 30]. A high-resolution transmission electron microscope (HR-TEM) (Talos L120C, Thermo Fisher Scientific) was used for particle size analysis. The aqueous solution of GO (5.0×10^{-5} kg/l) was dropped on carbon-coated copper grid and allow to dry for 12 hrs before TEM imaging. Scanning electron microscope (SEM) (Gemini, Carl Zeiss Microscopy) was used to demonstrate the coating of AuNPs and GO over fiber-ball structure. Energy-dispersive X-ray spectroscopy (EDX) was also used to identify the coated material over the fiber structure.

E. Coating of gold nanoparticles and graphene oxide over fiber ball structure

The AuNPs were immobilized over the micor-ball fiber structure as per method discussed in [26]. First, fibers were cleaned by three-step process using acetone, piranha solution and DI water. Thereafter, fibers were dipped in 1% ethanolic MPTMS solution for 12 hrs. The unbound MPTMS was removed by rinsed the fibers using ethanol and dried by nitrogen gas. Then, MPTMS-coated fibers were dipped in the AuNPs solution for 48 hrs. Again, unbound AuNPs were washed away using ethanol and dried by nitrogen gas.

The fiber balls were coated with GO using the method discussed in [29, 31]. The AuNPs-coated fibers were rinsed by DI water before GO coating. Thereafter, fibers were immersed in 3-(trimethoxysilyl)propyl methacrylate solution (silane agent) for 30 minutes. Then, it was kept in oven to dry at 70°C for 30 minutes for annealing process. GO was absorbed on the fiber balls using dip-coating method. The fibers were immersed in $4 \times 10^{-2}\ kg/l$ of prepared GO aqueous dispersion for 5 min. Thereafter, the fibers were placed in an oven at 70°C for a further 30 minutes to remove the organic residues and evaporate the solvent. The GO was immobilized over the fiber surface by the interactions of the π-π bonds of GO with the π bonds of silane agents [27]. The AuNPs-coated fibers were immersed in GO aqueous dispersion for three times for uniform thick coating over the fiber ball structure.

F. Uricase enzyme functionalization

Enzyme functionalization is a very important process for the fabrication of any enzymatic sensing probe as it enhanced the specificity of probe. This process was followed as discussed in [26]. The AuNPs/GO-coated micro-ball structures were rinsed by DI water and kept in ethanolic MUA solution (0.5 mM) for 5 hrs to produce the carboxylic group over sensor probe. Then, sensor probes were kept in EDC (200 mM)/NHS (50 mM) for 10 min to activate the carboxylic groups. Thereafter, fibers were dipped in the prepared uricase enzyme solution for 12 hrs for enzyme functionalization. Uricase enzyme solution (0.137 mg/ml) was prepared in 1 X PBS solution (pH 7.4) [8]. Due to the enzymatic nature of sensor, the fabricated fiber probes were kept in 2-8^{0}C refrigerator prior to use.

G. Preparation of uric acid solution

Finally, sensor probe application was characterized by different UA concentrations in the range of 10 µM to 1 mM because UA concentration in blood is reported to be in the range of 150 – 420 µM [8]. A stock solution of UA (1 mM) was prepared in 20 ml of 1 X PBS (pH 7.4) by heating the solution in a water bath using a magnetic stirrer at 90°C for 1 hr [8]. The different concentration of UA i.e., 900 µM, 800 µM, 700 µM, 600 µM, 500 µM, 400 µM, 300 µM, 200 µM, 100 µM, 50 µM, and 10 µM were prepared by diluting the stock solution in PBS solution. To check the selectivity of sensor probe, solution of other biomolecules such as D-glucose, glycine, L-alanine, L-proline, β-cyclodextrin, and L-glutathione were also prepared using PBS solution. These biomolecules are usually found along with UA in serum and urine. These serum samples were kept in 2-8 °C refrigerator and incubated at 37°C for 30 minutes prior to use [8].

H. Experimental setup

The measurement is very important for proper evaluation of any sensor structures. In this experiment, white light emitted from a tungsten-halogen light source (HL-2000, Ocean Optics Inc., USA) was used through a bifurcated optical fiber (SPLIT-400-VIS-NIR, Ocean Optics Inc., USA). Figure 3 shows the experimental setup for detection and measurement of UA. One end of the sensor probe was connected to the end of bifurcated optical fiber, and the other end with the sensing area was immersed into the UA solution. In this experiment, micro-ball fiber sensor structure is dipped into different UA concentrations ranging from 10 µM to 1 mM. Due to compact nature (350 µm size) of the sensor probe, a single drop of solution is enough for UA detection. The sensor probe was rinsed with PBS solution and dried after each measurement. As shown in Fig. 3, sensor probe is functionalized with the AuNPs, GO, and uricase that improves the sensitivity and selectivity of sensor probe. A USB2000+ spectrometer (Ocean Optics Inc., USA), was used as the detector. A computer with the OceanView software was connected to spectral data processing.

III. RESULTS AND ANALYSIS

A. Characterization of gold nanoparticles and graphene oxide

Primarily, AuNPs solution was characterized by using a UV-Vis spectrophotometer. The peak of the SPR wavelength was obtained at 519 nm as reported in Fig. 4a. The particle shape and size were obtained by the HR-TEM. TEM images (Fig. 4b) show that synthesized AuNPs are of spherical shape and ~11 nm in size (shown in inset of Fig. 4b). Further, an aqueous dispersion of GO was characterized by using UV-Vis spectrophotometer.

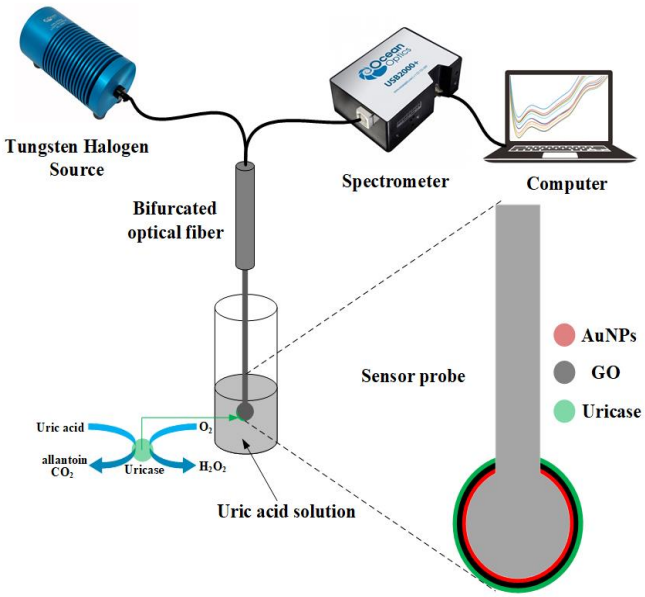

Fig. 3. Experimental setup for uric acid detection using a micro-ball fiber structure.

This article has been accepted for publication in a future issue of this journal, but has not been fully edited. Content may change prior to final publication. Citation information: DOI 10.1109/TNB.2019.2958891, IEEE Transactions on NanoBioscience

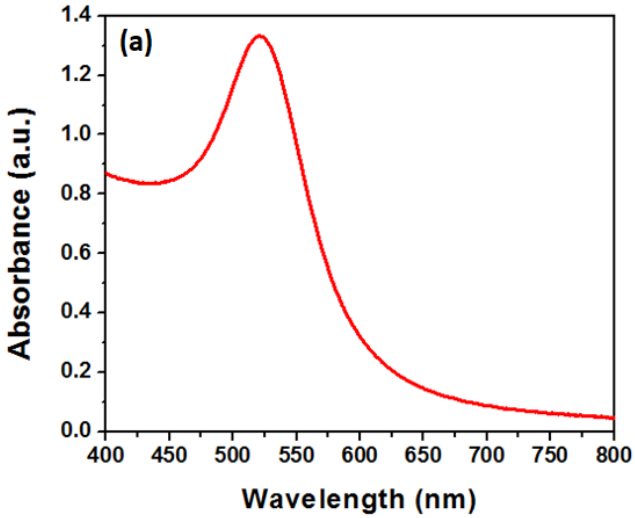

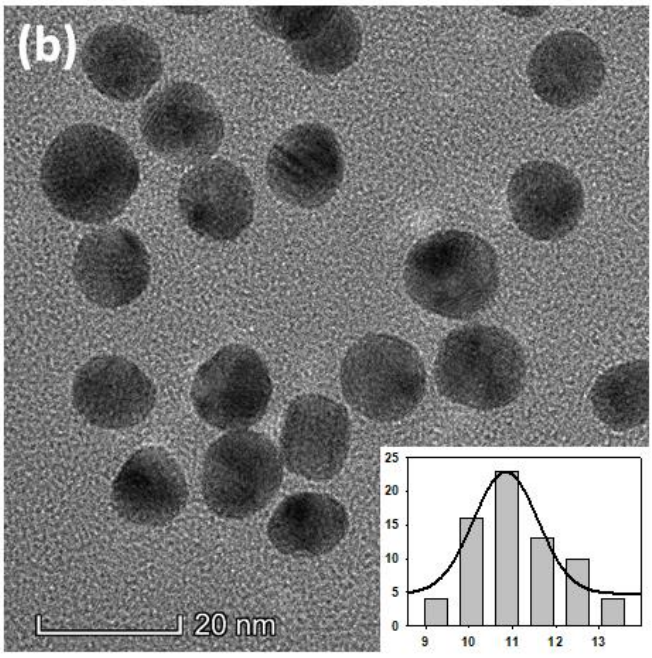

Fig. 4. (a) Absorbance spectrum of gold nanoparticles, (b) high-resolution transmission electron microscopic image of synthesized gold nanoparticles.

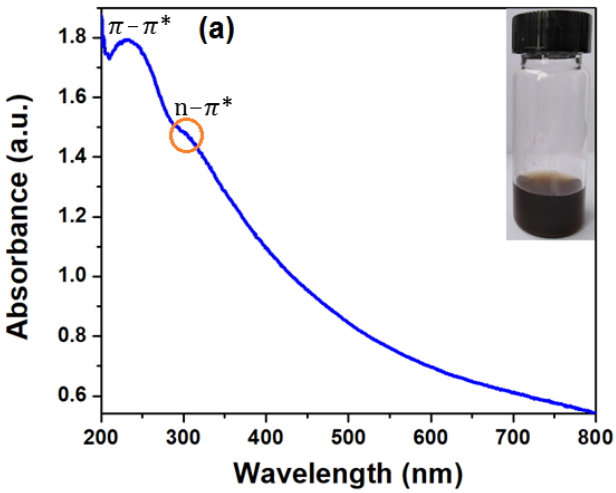

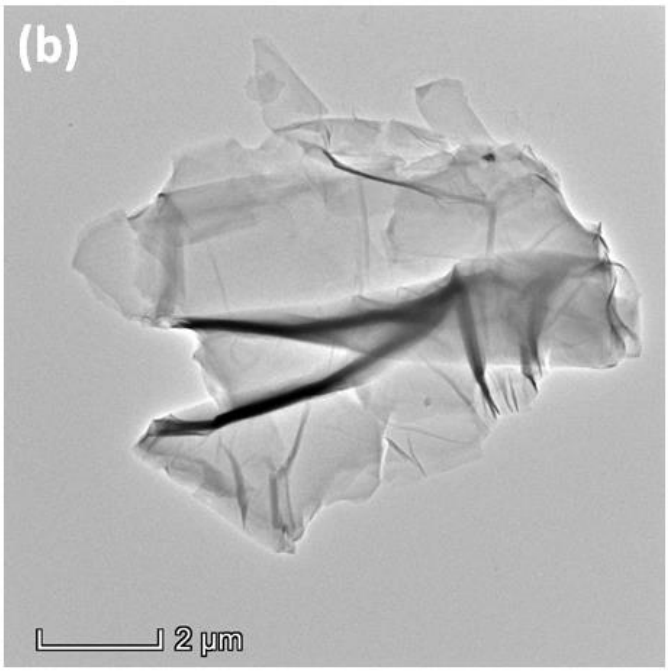

Fig. 5. (a) Absorbance spectrum of graphene oxide, (b) high-resolution transmission electron microscopic image of synthesized graphene oxide.

As shown in Fig. 5a, absorbance spectrum of GO solution displays two peaks at 310 nm and 230 nm which corresponds to n – π* transitions and π – π* transitions, respectively. The C – O bonds and nanoscale sp^2 of GO sheets are related to the 230 nm peak. It also shows that dispersed solution contains single-layered GO sheet as shown in HR-TEM image of Fig. 5b. The peak at 230 nm confirms the good quality of the synthesized GO powder and its aqueous dispersion [29].

B. Characterization of a sensor probe

The micro-ball sensor probe was characterized by scanning electron microscope (SEM) to investigate the coating of AuNPs and GO on the fiber structure. Figure 6a and 6c shows SEM images of the AuNPs-and GO/AuNPs-coated micro-ball fiber structure at lower magnification, respectively. These images displaying the complete structure of a sensor probe.

Figure 6b, 6d show the SEM images of sensor probe at higher magnification. These images together confirm that fiber micro-ball structure surface was uniformly coated with AuNPs and GO/AuNPs, respectively. Here, additional GO layer has enzyme binding capability over the fiber structure. Figures 6e and 6f show the thickness (around 100 nm) and dimensions (1-3 µm) of GO sheets coated over the fiber ball structure.

Fig. 7 shows the EDX of the AuNPs-and GO/AuNPs-coated micro-ball fiber structure. These results show that the only gold (Au) material is available over AuNPs-coated micro-ball fiber structure (shown in Fig. 7a), whether Au and carbon (C) materials are available over GO/AuNPs-coated micro-ball fiber structure (shown in Fig. 7b). It confirms that graphene sheets are attached over the AuNPs-layer.

C. Detection of uric acid solutions

An important parameter for the biosensing is response time that corresponds to the time required to detect and generate a stable

This article has been accepted for publication in a future issue of this journal, but has not been fully edited. Content may change prior to final publication. Citation information: DOI 10.1109/TNB.2019.2958891, IEEE Transactions on NanoBioscience

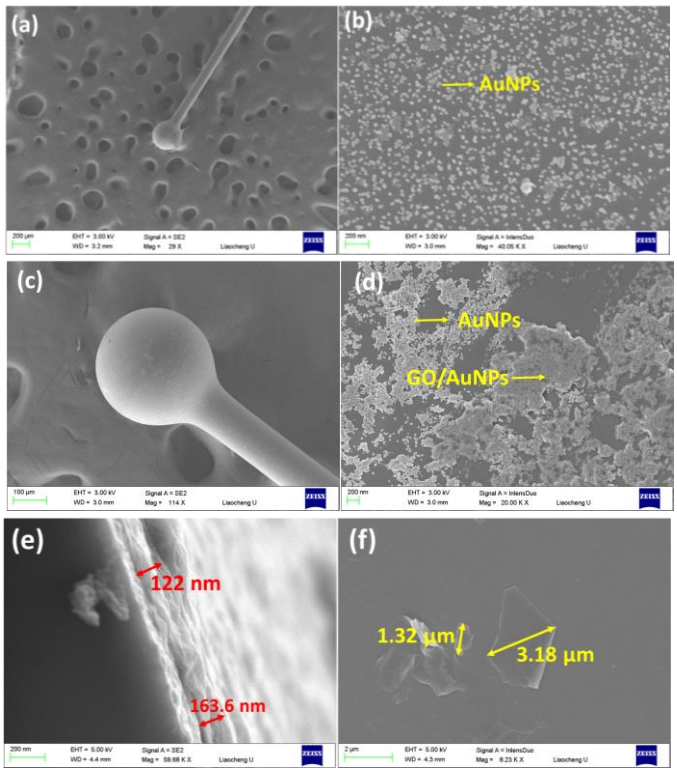

Fig. 6. Scanning electron microscopic (SEM) images of (a, b), uricase/AuNPs-coated micro-ball fiber structure, (c, d) uricase/GO/AuNPs-immobilized micro-ball fiber structure, (e) thickness of graphene oxide coating, and (f) dimension of graphene oxide flakes over micro-ball fiber structure.

result for a particular solution. The response time observed for the proposed sensor in the experimental set up is 20 min. Figures 8a and 8b shows the reflectance plot of uricase/AuNPs-coated and uricase/GO/AuNPs-coated micro-ball fiber structure, respectively. As the concentrations of UA solutions increases from 10 µM to 1 mM, the reflectance through sensor is decreases from 86.85 % to 86.76 % in the case of uricase/AuNPs-immobilized micro-ball fiber structure (shown in Fig. 8a),

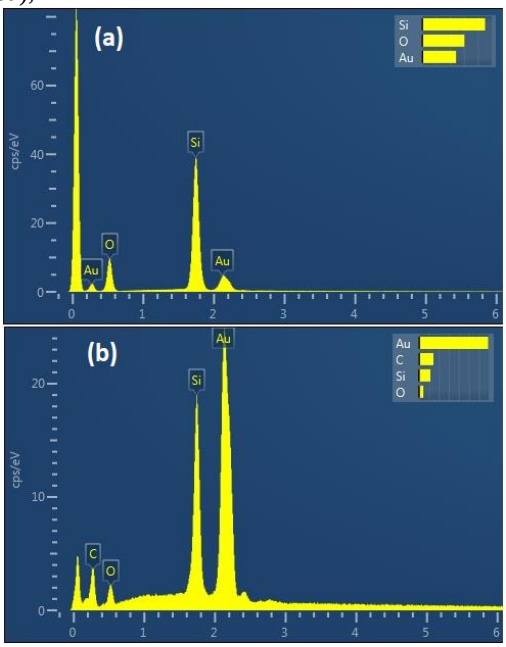

Fig. 7. Energy-dispersive X-ray spectroscopy (EDX) of (a) AuNPs-, (b) GO/AuNPs-coated micro-ball fiber structure.

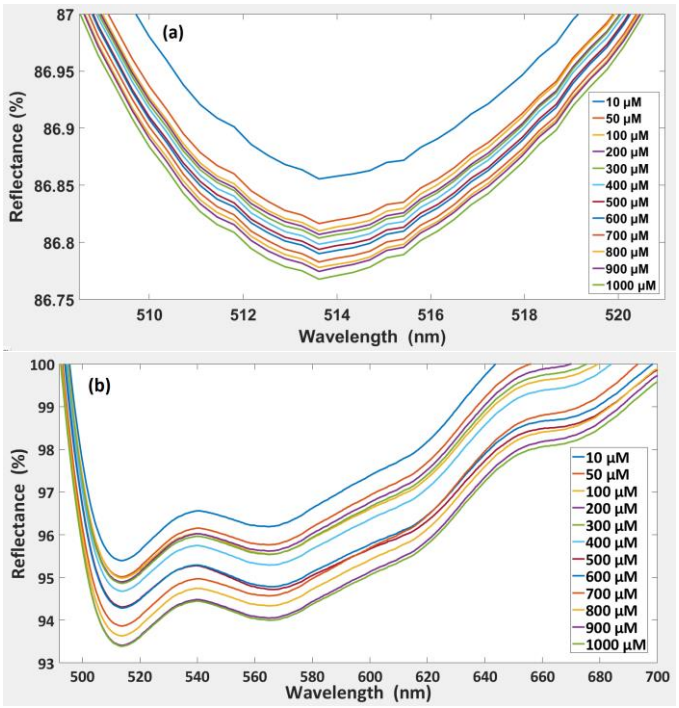

Fig. 8. Variation of reflectance against the different solutions of UA concentrations, (a) uricase/AuNPs -coated, (b) uricase/GO/AuNPs-coated micro-ball fiber structure.

and 95.39 % to 93.38 % in the case of uricase/GO/AuNPs-immobilized fiber micro-ball fiber structure (shown in Fig. 8b).

It can be concluded from the results that reflectance is inversely proportional to the UA concentrations. Here, LSPR phenomena occur due to AuNPs that vary the reflectance with different UA concentrations. The sensor response is due to the chemical reaction of uricase with UA. The uricase enzyme present over sensor structure converts the UA in the presence of oxygen into allantoin, carbon dioxide, and H_2O_2 (as shown Fig. 9). The level of H_2O_2 varies the RI over the surface of GO/AuNPs and varies the reflectance.

D. Reproducibility and reusability of a sensor probe

For reproducibility test, four different probes were fabricated with the optimized parameters and tested with the 1 mM UA solution. As shown in Fig. 10a, the reflectance of all the sensor probes are almost same for the 1 mM UA concentration. It shows that the sensor probe is reproducible.

For reusability test, three different UA concentrations (10 µM, 50 µM, and 400 µM) were considered. A new sensor probe was used to detect these UA concentrations. After detection, the sensor was rinsed with the PBS solution and kept in the refrigerator. The same UA concentrations were measured again using the same probe after 48 hrs to examine the reusability of the sensor probe. It can be observed from Fig. 10b that the sensor can be reused since reflectance of each measurement is almost similar. To know the reason for reproducibility and reusability of sensor probes, we have observed the surface of

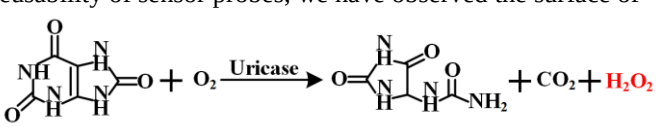

Fig. 9. Enzymatic reaction of uric acid in the presence of an uricase enzyme.

This article has been accepted for publication in a future issue of this journal, but has not been fully edited. Content may change prior to final publication. Citation information: DOI 10.1109/TNB.2019.2958891, IEEE Transactions on NanoBioscience

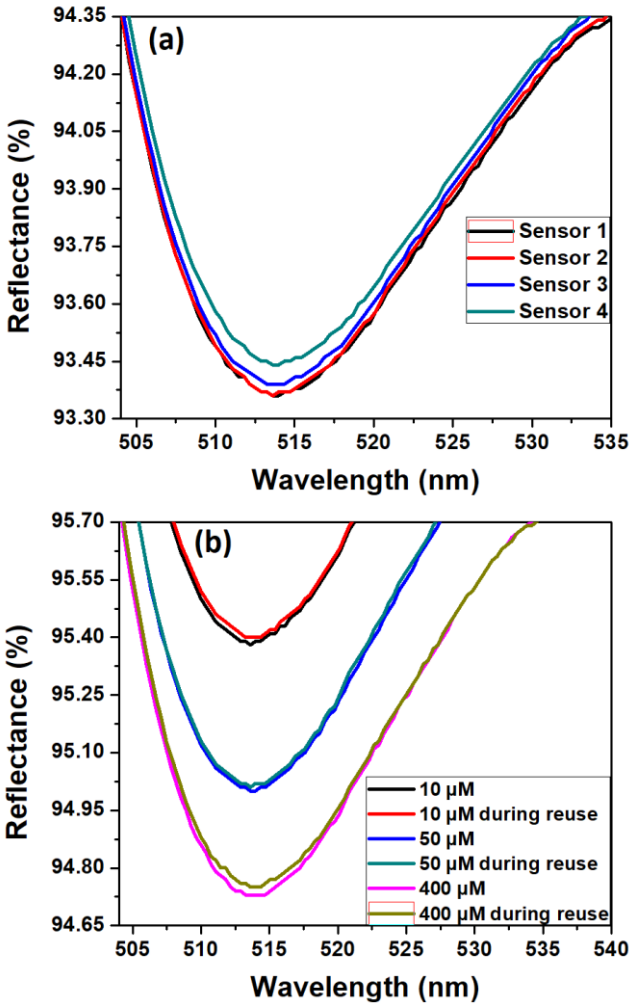

Fig. 10. (a) Reproducibility test of sensor probe using 1 mM uric acid solution, (b) reusability test of the proposed sensor using three different uric acid concentrations.

uricase/GO/AuNPs-coated sensor structure using SEM. Figure 11a shows the SEM image of sensor structure before UA measurement at 35.56 KX magnification. In this image, AuNPs were not visible due the MUA and enzyme coating. Figure 11b shows the SEM image of sensor structure after multiple measurements of UA at 9.01 KX magnification. The GO and AuNPs were still attached after multiple measurements of UA. The coating of nanomaterials is not removed due to the enzymatic reaction. Due to this reason, reproducibility and reusability of sensor are high.

E. Sensitivity, linearity and detection limit of sensor

Different UA concentrations were detected using the proposed sensor and result showed that the reflectance decreases with the increase in UA concentration. The variation of reflectance with the change in UA concentration was measured and plotted to calculate the sensitivity, linearity, and detection limit of the sensor. The curve fitting of the plot provides a linear regression equation i.e. R = -0.00005 C + 86.817 with the correlation coefficient (R^2 = 0.9928) in the case of uricase/AuNPs-immobilized sensor (as shown in Fig. 12a), and R = -0.0021 C + 95.366 with the correlation coefficient (R^2 = 0.9744) in the

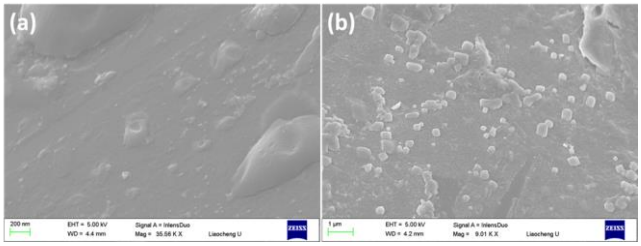

Fig. 11. SEM of uricase/GO/AuNPs -coated sensor (a) before, and (b) after uric acid measurement.

case of uricase/GO/AuNPs-immobilized sensor (as shown in Fig. 12b), where R is reflection (%) and C refers to the UA concentration in µM. As shown in Fig. 12a, the linearity range of the uricase/AuNPs -immobilized sensor is observed from 50 µM to 1 mM, whereas Fig. 12b shows the linearity range of the uricase/GO/AuNPs-coated micro-ball fiber structure in the range of 10 µM to 1 mM. The sensitivity of the proposed sensor from the linearity graph is observed as 0.005%/mM, and 2.1%/mM for uricase/AuNPs- and uricase/GO/AuNPs-coated micro-ball fiber structure, respectively. It has been concluded from the data that performance of uricase/GO/AuNPs-immobilized sensor is better than uricase/AuNPs-immobilized sensor. So, limit of detection (LoD) of the uricase/GO/AuNPs-immobilized sensor can be expressed as, LoD = (3×standard deviation)/sensitivity [11].

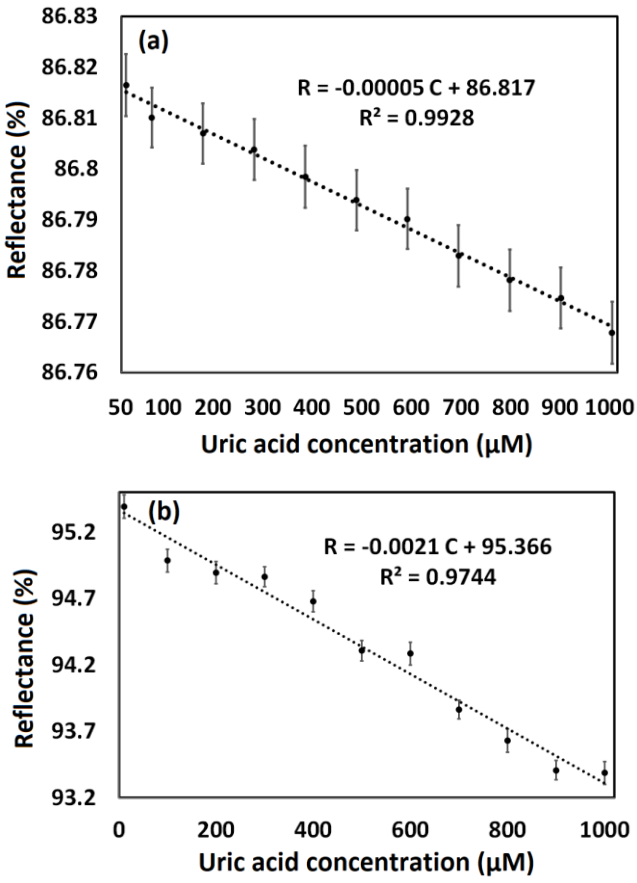

Fig. 12. Variation of reflectance with respect to uric acid concentration, (a) uricase/AuNPs-, (b) uricase/GO/AuNPs-coated micro-ball fiber structure.

This article has been accepted for publication in a future issue of this journal, but has not been fully edited. Content may change prior to final publication. Citation information: DOI 10.1109/TNB.2019.2958891, IEEE Transactions on NanoBioscience

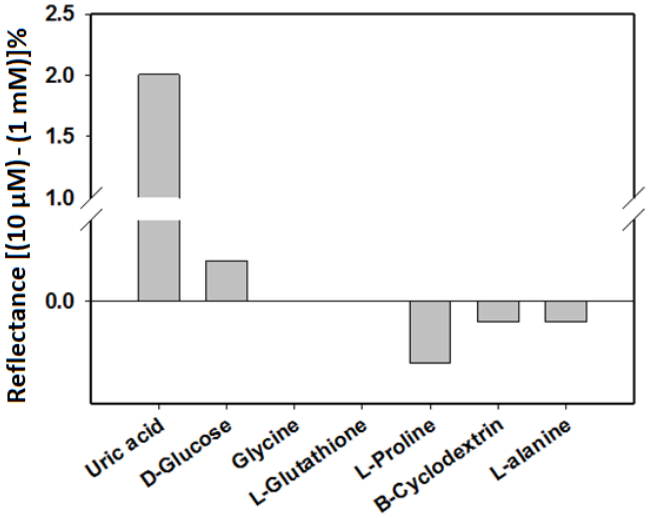

Fig. 13. Selectivity analysis of the proposed uric acid sensor using different interferents found with the uric acid.

The standard deviation of blank was calculated from considering 10-times measurement of PBS solution and is observed as 0.045925. Thus, the LoD of the proposed uricase/GO/AuNPs-immobilized sensor is obtained as 65.60 µM.

F. Selectivity of sensor

Selectivity test was performed to examine the specificity of the developed sensor with different other biomolecules such as D-glucose, glycine, L-glutathione, L-proline, β-cyclodextrin, and L-alanine which are normally present in serum/urine. As per linearity range of uricase/GO/AuNPs-immobilized sensor probe, two concentrations (10 µM and 1 mM) of these interferents were tested for selectivity measurement. The shift in reflectance from lower concentration to a higher concentration of these interferents is shown using bar graph in Fig. 13. It can be observed from the results that there is no significant shift in the reflectance intensity of probe when it is incubated with other interferents. As shown in Fig. 13, reflectance shift is higher in the case of UA due to presence of uricase enzyme over surface. Further, it proves that synthesized probe is specific for UA detection.

G. Analysis of uric acid in human serum

To know the practical application of sensor, it could be applied for the measurement of UA in clinical samples [3, 6-8]. We have measured the UA concentration in five human serum samples, which have been collected from human blood samples donated by Liaocheng People's Hospital associated with Medical College of Liaocheng University, China. To extract the serum, blood samples were first centrifuged at 4000 rpm for 5 min and supernatant was removed and filtered using a 45-micron syringe filter to get the light-yellow serum [8]. The linear range of uricase/GO/AuNPs-coated micro-ball fiber sensor is reported in the wide range of 10 µM to 1 mM. Thus, human serum samples have been tested directly without another pretreatment. The same measurement setup and parameters have been used for serum samples, only serum has been used in the place of UA solution.

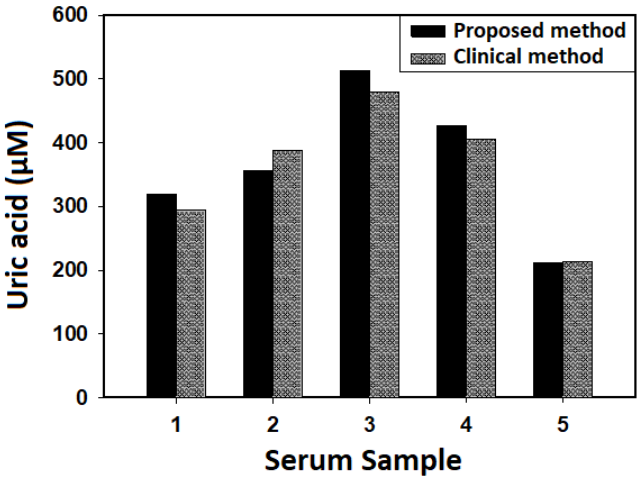

Fig. 14. Analytical results of uric acid in human serum obtained using proposed uricase/GO/AuNPs-immobilized sensor and A5800 Automatic Biochemical Analyzer.

At the same time, A5800 Automatic Biochemical Analyzer was used to determine the UA concentration and to test the accuracy of the proposed method. Figure 14 shows the results obtained from the developed sensor and clinical results of A5800 Automatic Biochemical Analyzer. The relative error (%) of our method is 7.83, -8.98, 6.62, 5.15, and -0.94 for the five clinical samples of 294 µM, 388 µM, 479 µM, 405 µM, and 214 µM, respectively. The data shown in graph indicated that our proposed method is reliable for clinical diagnosis.

H. Performance analysis of proposed sensor with existing sensors

Various UA biosensors based on electrochemical, colorimetric, fluorescence have been reported, till date. A comparison of performance between the proposed sensor and several uricase based sensors are summarized in Table 1.

Table 1. Performance analysis of proposed sensor with existing sensors.

Material used	Mechanism used	Linear range	Detection Limit	Sensitivity	Ref.
Cu_2ZnSnS_4 NPs	Electrochemical	0 - 700 µM	0.066 µM	n.r.[a]	[2]
$HAuCl_4$	Colorimetric	0.001- 80 µM	0.67 nM	n.r.[a]	[5]
Au/Ag NCs	Fluorescence	5 - 50 µM	5.1 µM	n.r.[a]	[7]
AuNCs	Fluorescence	0.7- 80 µM	120 nM	n.r.[a]	[3]
AuNCs	Fluorescence	10 - 800 µM	6.6 µM	n.r.[a]	[6]
ZnO nanowires	SPR technique	0 - 500 ppm	5.74%	0.001 nm/%	[9]
Ag NCs	Chemilumine scence	2 - 100 µM	0.75 µM	n.r.[a]	[11]
AgNPs	LSPR technique	0 - 50 μMdm^{-3}	5 μMdm^{-3}	n.r.[a]	[8]
ZnO nanostructures	SPR technique	0 - 500 ppm	5.6 ppm*	0.0025 mV/ppm	[13]
AuNPs	LSPR technique	50 µM - 1 mM	n.r.[a]	0.005 %/mM	This work
AuNPs/GO	LSPR technique	10 µM - 1 mM	65.60 µM	2.1%/ mM	

[a] not reported. *Conversion (1 ppm = 1000 µg/ L; $M.W._{UA}$ = 168.11g/mole)

It can be observed that linearity range and detection limit of the previously reported sensors are not enough to detect the higher concentration of UA in serum. It needs to dilute the samples several times that may affect the results. In this work, uricase/GO/AuNPs-functionalized micro-ball fiber sensor has been used for the UA detection that exhibits a wide linearity range, low detection limit, high sensitivity, and selectivity performances.

IV. Conclusion

A sensor using an uricase/GO/AuNPs functionalized micro-ball fiber sensor has been developed for UA detection in the micromolar range. In this experiment, proposed sensors are used to measure the different UA concentrations ranging from 10 µM to 1 mM. The sensor works on the principle of surface plasma property and localized surface plasmon resonance. AuNPs and GO were synthesized and characterized for this work. The absorbance spectrum of AuNPs and GO were 519 nm and 230 nm, respectively that confirms the synthesis of a better quality of nanomaterials. The presence of AuNPs and GO enhanced the sensitivity of fabricated sensors. The specificity of the sensor has been increased by the uricase enzyme that reacted with the UA and produces the H_2O_2 and thus changed the reflectance. Thus, the linearity range of the sensor is 10 µM – 1 mM of UA concentrations with sensitivity 2.1 %/mM. The detection limit of the proposed sensor is 65.60 µM. So, the developed sensor is able to detect the lower and higher concentration of UA in human serum because normal range of UA concentration is in the range of 150 – 420 µM. The clinical samples were also tested using proposed method and A5800 Automatic Biochemical Analyzer. The results of the developed sensor are consistent with the results of A5800 Automatic Biochemical Analyzer. It shows that proposed sensor can be successfully used for UA detection in human serum samples. Due to micro-size sensor probe, it has ability to detect a single drop of UA solution. Overall, proposed sensor has good linearity range, low detection limit, low cost, high accuracy, and also found to be highly sensitive and selective.

References

[1] L. Liu, L. Liu, Y. Wang, and B.-C. Ye, "A novel electrochemical sensor based on bimetallic metal–organic framework-derived porous carbon for detection of uric acid," *Talanta,* vol. 199, pp. 478-484, 2019/07/01/, 2019.

[2] S. Jain, S. Verma, S. P. Singh, and S. N. Sharma, "An electrochemical biosensor based on novel butylamine capped CZTS nanoparticles immobilized by uricase for uric acid detection," *Biosensors and Bioelectronics,* vol. 127, pp. 135-141, 2019/02/15/, 2019.

[3] P. Xu, R. Li, Y. Tu, and J. Yan, "A gold nanocluster-based sensor for sensitive uric acid detection," *Talanta,* vol. 144, pp. 704-709, 2015/11/01/, 2015.

[4] B. J. Matsoso, B. K. Mutuma, C. Billing, K. Ranganathan, T. Lerotholi, G. Jones, and N. J. Coville, "Investigating the electrochemical behaviour and detection of uric acid on ITO electrodes modified with differently doped N-graphene films," *Journal of Electroanalytical Chemistry,* vol. 833, pp. 160-168, 2019/01/15/, 2019.

[5] J. Wang, X. Fang, Y. Zhang, X. Cui, H. Zhao, X. Li, and Z. Li, "A simple and rapid colorimetric probe for uric acid detection based on redox reaction of 3,3′,5,5′-tetramethylbenzidine with HAuCl4," *Colloids and Surfaces A: Physicochemical and Engineering Aspects,* vol. 555, pp. 565-571, 2018/10/20/, 2018.

[6] J. Wang, Y. Chang, W. B. Wu, P. Zhang, S. Q. Lie, and C. Z. Huang, "Label-free and selective sensing of uric acid with gold nanoclusters as optical probe," *Talanta,* vol. 152, pp. 314-320, 2016/05/15/, 2016.

[7] X.-y. Wang, G.-b. Zhu, W.-d. Cao, Z.-j. Liu, C.-g. Pan, W.-j. Hu, W.-y. Zhao, and J.-f. Sun, "A novel ratiometric fluorescent probe for the detection of uric acid in human blood based on H2O2-mediated fluorescence quenching of gold/silver nanoclusters," *Talanta,* vol. 191, pp. 46-53, 2019/01/01/, 2019.

[8] N. Misra, V. Kumar, L. Borde, and L. Varshney, "Localized surface plasmon resonance-optical sensors based on radiolytically synthesized silver nanoparticles for estimation of uric acid," *Sensors and Actuators B: Chemical,* vol. 178, pp. 371-378, 2013/03/01/, 2013.

[9] A. Lokman, S. W. Harun, Z. Harith, H. A. Rafaie, R. M. Nor, and H. Arof, "Inline Mach–Zehnder interferometer with ZnO nanowires coating for the measurement of uric acid concentrations," *Sensors and Actuators A: Physical,* vol. 234, pp. 206-211, 2015/10/01/, 2015.

[10] M. Batumalay, S. W. Harun, F. Ahmad, R. M. Nor, N. R. Zulkepely, and H. Ahmad, "Tapered Plastic Optical Fiber Coated With Graphene for Uric Acid Detection," *IEEE Sensors Journal,* vol. 14, no. 5, pp. 1704-1709, 2014.

[11] L. Rana, R. Gupta, M. Tomar, and V. Gupta, "Highly sensitive Love wave acoustic biosensor for uric acid," *Sensors and Actuators B: Chemical,* vol. 261, pp. 169-177, 2018/05/15/, 2018.

[12] A. K. Sharma, A. K. Pandey, and B. Kaur, "A Review of advancements (2007–2017) in plasmonics-based optical fiber sensors," *Optical Fiber Technology,* vol. 43, pp. 20-34, 2018/07/01/, 2018.

[13] M. Batumalay, Z. Harith, H. A. Rafaie, F. Ahmad, M. Khasanah, S. W. Harun, R. M. Nor, and H. Ahmad, "Tapered plastic optical fiber coated with ZnO nanostructures for the measurement of uric acid concentrations and changes in relative humidity," *Sensors and Actuators A: Physical,* vol. 210, pp. 190-196, 2014/04/01/, 2014.

[14] X. Wang, Z. Li, J. Lai, X. Tang, and P. Qiu, "Sensitive and Highly Selective Biosensor Based on Triangular Au Nanoplates for Detection of Uric Acid in Human Serum," *Chemistry Africa,* vol. 1, no. 1, pp. 29-35, 2018/06/01, 2018.

[15] S. Kumar, R. Singh, B. K. Kaushik, N. Chen, Q. S. Yang, and X. Zhang, "LSPR-Based Cholesterol Biosensor Using Hollow Core Fiber Structure," *IEEE Sensors Journal,* vol. 19, no. 17, pp. 7399-7406, 2019.

[16] J. Shah, R. Purohit, R. Singh, A. S. Karakoti, and S. Singh, "ATP-enhanced peroxidase-like activity of gold nanoparticles," *Journal of Colloid and Interface Science,* vol. 456, pp. 100-107, 2015/10/15/, 2015.

[17] S. Kumar, R. Singh, B. K. Kaushik, N. Chen, Q. S. Yang, and X. Zhang, "LSPR based cholesterol biosensor using hollow core fiber structure," *IEEE Sensors Journal,* pp. 1-1, 2019.

[18] Y. Zhao, X.-g. Li, X. Zhou, and Y.-n. Zhang, "Review on the graphene based optical fiber chemical and biological sensors," *Sensors and Actuators B: Chemical,* vol. 231, pp. 324-340, 2016/08/01/, 2016.

[19] S. W. Harun, A. A. Jasim, H. A. Rahman, M. Z. Muhammad, and H. Ahmad, "Micro-Ball Lensed Fiber-Based Glucose Sensor," *IEEE Sensors Journal,* vol. 13, no. 1, pp. 348-350, 2013.

[20] A. A. Jasim, A. Z. Zulkifli, M. Z. Muhammad, S. W. Harun, and H. Ahmad, "A new compact micro-ball lens structure at the cleaved tip of microfiber coupler for displacement sensing," *Sensors and Actuators A: Physical,* vol. 189, pp. 177-181, 2013/01/15/, 2013.

[21] C. Song, P. L. Gehlbach, and J. U. Kang, "Ball Lens Fiber Optic Sensor based Smart Handheld Microsurgical Instrument," *Proceedings of SPIE--the International Society for Optical Engineering,* vol. 8576, pp. 10.1117/12.2004947, 2013.

[22] S. S. Fuglerud, K. Milenko, I. L. Jernelv, A. Aksnes, R. Ellingsen, and D. R. Hjelme, "A miniaturized ball-lensed fiber optic NIR transmission spectroscopy-based glucose sensor," *OSA Technical Digest (online).* p. SeM3E.5.

[23] R. Gravina, G. Testa, and R. Bernini, "Perfluorinated plastic optical fiber tapers for evanescent wave sensing," *Sensors (Basel, Switzerland),* vol. 9, no. 12, pp. 10423-10433, 2009.

[24] H. Li, H. Li, F. Meng, X. Lou, and L. Zhu, "All-fiber MZI sensor based on seven-core fiber and fiber ball symmetrical structure," *Optics and Lasers in Engineering*, vol. 112, pp. 1-6, 2019/01/01/, 2019.

[25] S. P. Dash, S. K. Patnaik, and S. K. Tripathy, "Investigation of a low cost tapered plastic fiber optic biosensor based on manipulation of colloidal gold nanoparticles," *Optics Communications*, vol. 437, pp. 388-391, 2019/04/15/, 2019.

[26] S. Kumar, B. K. Kaushik, R. Singh, N.-K. Chen, Q. S. Yang, X. Zhang, W. Wang, and B. Zhang, "LSPR-based cholesterol biosensor using a tapered optical fiber structure," *Biomedical Optics Express*, vol. 10, no. 5, pp. 2150-2160, 2019/05/01, 2019.

[27] G. Sobon, J. Sotor, J. Jagiello, R. Kozinski, M. Zdrojek, M. Holdynski, P. Paletko, J. Boguslawski, L. Lipinska, and K. M. Abramski, "Graphene Oxide vs. Reduced Graphene Oxide as saturable absorbers for Er-doped passively mode-locked fiber laser," *Optics Express*, vol. 20, no. 17, pp. 19463-19473, 2012/08/13, 2012.

[28] V. Semwal, and B. D. Gupta, "LSPR- and SPR-Based Fiber-Optic Cholesterol Sensor Using Immobilization of Cholesterol Oxidase Over Silver Nanoparticles Coated Graphene Oxide Nanosheets," *IEEE Sensors Journal*, vol. 18, no. 3, pp. 1039-1046, 2018.

[29] K. P. W. Dissanayake, W. Wu, H. Nguyen, T. Sun, and K. T. V. Grattan, "Graphene-Oxide-Coated Long-Period Grating-Based Fiber Optic Sensor for Relative Humidity and External Refractive Index," *Journal of Lightwave Technology*, vol. 36, no. 4, pp. 1145-1151, 2018.

[30] M. Divagar, A. Gowri, S. John, and V. V. R. Sai, "Graphene oxide coated U-bent plastic optical fiber based chemical sensor for organic solvents," *Sensors and Actuators B: Chemical*, vol. 262, pp. 1006-1012, 2018/06/01/, 2018.

[31] A. A. Shabaneh, S. H. Girei, P. T. Arasu, W. B. W. A. Rahman, A. A. A. Bakar, A. Z. Sadek, H. N. Lim, N. M. Huang, and M. H. Yaacob, "Reflectance response of tapered optical fiber coated with graphene oxide nanostructured thin film for aqueous ethanol sensing," *Optics Communications*, vol. 331, pp. 320-324, 2014/11/15/, 2014.

Santosh Kumar (S'12–M'15-SM'19) received the Ph.D. degree from the Indian Institute of Technology (Indian School of Mines), Dhanbad, India.

He is currently an Associate Professor with the School of Physics Science and Information Technology, Liaocheng University, Liaocheng, China. His current research interests include photonics devices based on Mach-Zehnder interferometer, photonics crystal fiber, fiber Bragg grating, and optical fiber-based biosensors. He is a Senior Member of IEEE and SPIE.

Ragini Singh received the Ph.D. degree from Ahmedabad University, Ahmedabad, India, in 2018.

She is currently an Assistant Professor with the School of Agriculture Science, Liaocheng University, Liaocheng, China. Her current research interests include nanotechnology, molecular biology, environmental biology, and immunology.

Guo Zhu received a Bachelor's degree from Liaocheng University, Liaocheng, China, in year 2018, where he is currently pursuing a master's degree. His current research interests are optical fiber-based biosensors.

Qingshan Yang received a Bachelor's degree in engineering from Liaocheng University, Liaocheng, China, in 2017, where he is currently pursuing a master's degree. His current research interests are optical fiber-based biosensors.

Xia Zhang received the Ph.D. degree in optical engineering from the Beijing University of Posts and Telecommunications, Beijing, in 2016.

She is currently an Associate Professor at Liaocheng University, China. Her research areas are high-speed optical communications and optoelectronics.

Shuang Cheng received a Bachelor's degree from Henan Industry University in 1994 and got a Ph.D. degree from Tianjin Institute of Hygiene in 2005. Currently, he is a Professor at the School of Agriculture, Liaocheng University, China.

His current research interests included functional drugs and food ingredients discovery.

Bingyuan Zhang received his doctor's degree in January 2008 from Beijing University of Technology. Currently, he is working as a Professor at Liaocheng University, China.

His current research interest is in experimental physics, Lasers, and Optical fiber-based biosensors.

Brajesh Kumar Kaushik (S'07–M'09–SM'13) received the Ph.D. degree from the Indian Institute of Technology Roorkee, at Roorkee, India, in 2007.

He is currently an Associate Professor with the Department of Electronics and Communication Engineering, Indian Institute of Technology Roorkee. His current research interests include high-speed interconnects, low-power very large scale integration design, memory design, carbon nanotube-based designs, organic electronics, FinFET device circuit co-design, electronic design automation, spintronics based devices, circuits, and computing, image processing, and optics- and photonics-based devices.

Fengzhen Liu received a Ph.D. degree from Chinese Academy of Sciences University in 2014. In 2015, she did postdoctor at Tsinghua University. In 2016, she was visiting scholar at University of British Columbia of Canada. In 2017, she was the director of Institute for biomaterials laboratory and Deputy Director of scientific research department, Liaocheng People's Hospital. In 2019，she got Hospital leadership and management certificate at Harvard Medical School. She published more than 20 SCI papers and 3 patents so far, got more than 10 projects and 5 rewards. She is American Science and Technology Life Member, Journal of Cardiovascular Research and Medicine Editor member, Chinese Society for Biomaterials-Smart Biomaterials Committee Member, Chinese Society for Biomaterials-Bone Repair Materials and Equipment Committee Member, China Medicine Education Association-Medical Science Promotion Committee Member, Chinese Stomatological Association-Dental Materials Professional Committee Member.

Her research interests include bone regeneration and immunity.